A Thermodynamic Database for Copper Smelting and Converting

SERGEI A. DEGTEROV and ARTHUR D. PELTON

The thermodynamic properties of the slag, matte, and liquid copper phases in the Cu-Ca-Fe-Si-O-S system have been critically assessed and optimized over the ranges of compositions of importance to copper smelting/converting based on thermodynamic and phase equilibria information available in the literature and using the modified quasichemical model. A thermodynamic database has been developed, which can be used for the calculation of matte-slag-copper-gas phase equilibria of interest for the production of copper. The model reproduces within experimental error limits all available experimental data on phase diagrams, matte-alloy miscibility gap and tie-lines, enthalpies of mixing, and activities of Cu and S in the matte and liquid alloy. The calculated solubilities of Cu in both S-free slag and slag equilibrated with matte are also in good agreement with experiment under all studied conditions, such as at SiO_2 saturation, in equilibrium with Fe, Cu, or Cu-Au alloys, at fixed oxygen or SO_2 partial pressures and at different contents of CaO in the slag. Sulfide contents (sulfide capacities) of the slags are predicted within experimental error limits from the modified Reddy–Blander model, with no adjustable parameters. As an example of the application of the database, the stability field of matte/slag equilibrium is calculated, and the matte and slag compositions are plotted *vs* iron to silica ratio in the slag at various SO_2 pressures over this field. The matte-slag two-phase field is limited by the calculated lines corresponding to precipitation of copper, silica, and magnetite.

I. INTRODUCTION

THE present study is concerned with the development of thermodynamic models and a thermodynamic database of model parameters for the matte, slag, and blister copper phases in the Cu-Ca-Fe-Si-O-S system. When used with the Gibbs energy minimization software and other databases of the FACT thermodynamic computing system, these databases will permit the calculation of matte-slag-copper-gas phase equilibria that take place during copper smelting and converting.

In particular, the copper, sulfur, and magnetite contents of the slag can be accurately calculated over wide ranges of temperature, iron to silica ratio, percentage of lime, and oxygen potential. The solubility of iron in the matte as well as that of sulfur, iron, and oxygen in blister copper can also be computed. Furthermore, one can calculate liquidus temperatures and conditions for precipitation of solid phases from the slag. All these calculations can be readily used to develop a better understanding of modern smelting and converting processes and to optimize the operating conditions.

It should be noted that direct experimental study of the gas-matte-slag-copper equilibria is subject to experimental errors because of the complexity of the system and because of problems with sampling, quenching, and analysis of the phases. Entrainment of matte in the slag can also affect the accuracy of measurements.[1] Taking into account the fact that operating conditions of most smelters and converters are not far from equilibrium,[2] one can expect calculations to be as accurate as or, in certain cases, even more accurate than direct experiments because they are based on experimental data of good quality obtained for less complex subsystems, which are much easier to study. For example, the difference between the measured losses of copper in the slag and the calculated copper solubility will represent the amount of entrained copper.

Under conditions of interest for copper smelting and converting, the concentrations of Ca and Si in the matte and liquid copper alloy are very small. Hence, the presence of these components was neglected. The oxygen content in the matte is reported[3,4,5] to decrease with increasing matte grade (wt pct Cu in the matte). For example, the oxygen concentration is about 1.1 $\pm$ 0.2, 0.8 $\pm$ 0.2, and 0.2 $\pm$ 0. 1 wt pct for 50, 60, and 78 wt pct Cu in the matte, respectively. The matte grade is normally higher than 50 wt pct Cu in present day plant practice. Therefore, the presence of oxygen will have only a small effect on the matte-slag-copper-gas equilibria considered in the present study. Consequently, oxygen was not taken into account in the matte model.

Oxygen impurity in blister copper after converting may be of some importance, and so oxygen was taken into account as a component of the liquid copper model. All six components of the Cu-Ca-Fe-Si-O-S system were considered for the slag model. Gold was also incorporated into the liquid copper model in order to treat numerous experimental data on matte/slag/Cu-Au-alloy equilibria discussed subsequently.

The modified quasichemical model[6–9] is used to describe the thermodynamic properties of slag, matte, and liquid copper alloy. Strictly speaking, there is just one liquid phase in this system with miscibility gaps. Under certain conditions, which are far from those used in copper smelting and converting, these phases completely dissolve in each other. In the present study, however, slag, matte, and alloy are treated as separate phases. This is sufficient for thermodynamic

SERGEI A. DEGTEROV, Senior Research Associate, and ARTHUR D. PELTON, Professor of Metallurgy, are with the Centre de Recherche en Calcul Thermochimique, Ecole Polytechnique de Montreal, Montreal, PQ, Canada H3C 3A7.

Manuscript submitted August 10, 1998.

Table I. The Thermodynamic Properties of the Liquid Copper Phase

Pure Component	Reference for G^o	Stability Parameter, J/mol
Cu (liquid)	14	—
Fe (liquid)	14	—
S (liquid)	15	—
Au (liquid)	14	—
$^1/_2O_2$ (gas)	14	10,460
Excess Parameters	**Value, J/mol**	
$\omega^{00}_{\text{Cu-Fe}}$	19,863 − 4.000 T	
$\omega^{01}_{\text{Cu-Fe}}$	10,000	
$\omega^{03}_{\text{Cu-Fe}}$	750	
$\omega^{00}_{\text{Cu-S}}$	−24,183	
$\omega^{01}_{\text{Cu-S}}$	−39,351	
$\omega^{00}_{\text{Fe-S}}$	−34,181 + 2.789 T	
$\omega^{01}_{\text{Fe-S}}$	−26,681	
$\omega^{02}_{\text{Fe-S}}$	−24,230	
$\omega^{00}_{\text{Au-Cu}}$	−12,677 − 3.239 T	
$\omega^{01}_{\text{Au-Cu}}$	9703	
$\omega^{02}_{\text{Au-Cu}}$	−9664	
$\omega^{00}_{\text{Cu-O}}$	−10,033	
$\omega^{01}_{\text{Cu-O}}$	−20,920	
$\omega^{001}_{\text{Cu-S(Fe)}}$	3766	

modeling of copper smelting and converting. A description of the thermodynamic properties of all three phases by one set of model equations will be the subject of future work.

The Reddy-Blander model, modified by Pelton *et al.*,[10] is used to model the sulfide solubility in the slag.

The thermodynamic database has been developed by critical evaluation and optimization of literature data. In a thermodynamic "optimization," all available thermodynamic and phase equilibrium data for a system are evaluated simultaneously in order to obtain one set of model equations for the Gibbs energies of all phases as functions of temperature and composition. From these equations, all of the thermodynamic properties and the phase diagram can be back-calculated. In this way, all the data are rendered self-consistent and consistent with thermodynamic principles. Thermodynamic property data, such as activity data, can aid in the evaluation of the phase diagram, and phase diagram measurements can be used to deduce thermodynamic properties. Discrepancies in the available data can often be resolved, and interpolations and extrapolations can be made in a thermodynamically correct manner. A small set of model parameters is obtained. This is ideal for computer storage and calculation of properties and phase diagrams.

II. Cu-Fe, Cu-S, Fe-S, AND Cu-Fe-S SYSTEMS

For the present study, two phases in the Cu-Fe system are important: the liquid and the γFe-based solid solution. The latter is necessary to deal with experimental data on matte-slag equilibria at γFe saturation. Thermodynamic properties of the Cu-Fe system have been reviewed and assessed.[11,12] Experimental data selected from these assessments were used[13] to obtain the three $\omega^{ij}_{\text{Cu-Fe}}$ parameters of the modified quasichemical model for the liquid alloy, which are listed in Table I, where the notation of the quasichemical model as described in References 7 through 9 is used. The parameters Z_{Cu}, Z_{Fe}, and Z_{S} of the model are 2.7548, 5.5098, and 5.5098, respectively. The Gibbs energies of pure liquid iron and copper were taken from the FACT database[14] and that of pure liquid sulfur from Sharma and Chang.[15]

The regular solution model has been used to describe the properties of the γFe-based solid solution. Two parameters of the model were obtained from the phase diagram data:[16–20]

$$G^E = X_{\text{Cu}}X_{\text{Fe}}\,(42{,}177 - 7.078T)\ \text{J/mol}$$

The measurements of the enthalpy of mixing[21–24] and the activity of copper[25] in the Cu-Fe liquid indicate positive deviations from ideality. All these data and the phase diagram[16–20] are reproduced within experimental error limits by the model.

The sulfur activity data in the metal-rich region of the Cu-S system[26–29] number more than 130 and are somewhat dispersed but generally in agreement. The measurements[26,27,30–34] of the miscibility gap between matte and alloy are scattered but are generally consistent except for the data of Moulki and Osterwald,[34] which indicate a lower consolute temperature than the others.

The sulfur activity data in the metal-rich region of the Fe-S system[35–38] are scattered. In the optimization, more weight was assigned to the sulfur activity data measured in an induction furnace (Sherman *et al.*,[39] 1550°C; Ishii and Fuwa,[40] 1550°C and 1600°C) and in a resistance furnace (Ban-ya and Chipman[41] and Alcock and Cheng,[36] 1550°C), which are respectively in good agreement.

These data were optimized,[13] and the two $\omega^{ij}_{\text{Cu-S}}$ and three $\omega^{ij}_{\text{Fe-S}}$ parameters of the quasichemical model listed in Table I were obtained. The model describes all the data within experimental uncertainty.

The binary optimizations for the matte in the Cu-S and Fe-S systems are taken from Kongoli *et al.*[42] The modified quasichemical model[6] describes the short-range ordering for molten sulfide mattes, which is considered to result from the fact that metal-sulfur nearest-neighbor pairs are energetically favored over metal-metal and sulfur-sulfur pairs. Using only binary parameters, the model predicts the thermodynamic properties of Fe-Cu-S mattes over a wide range of composition and temperature within experimental error limits.[42]

It is important to describe particularly well the matte-alloy phase boundaries and the sulfur activity in the matte-alloy two-phase field in the Cu-S system.[26] These data essentially fix the sulfur potential and the concentration of sulfur in liquid copper for the matte-slag-copper-gas equilibria in copper converters. A better fit was achieved by using slightly different standard state properties of liquid copper in the matte phase as compared to the earlier work.[42] The optimized value of the stability parameter, which is added to the Gibbs energy of pure liquid copper taken from JANAF,[43] is 6130 J/mol compared to a value of (16,547 − 7.681T) J/mol in the earlier optimization. This correction does not affect the sulfur activities in the matte optimized by Kongoli *et al.*[42] Experimental and calculated values for the copper-matte two-phase field are compared in Table II.

As was mentioned previously, a separate solution, different from the matte phase, is used for the Cu-Fe alloy. The Cu-Fe binary interaction parameters for the matte solution have only a very small effect on the properties of the matte

Table II. Sulfur Content of Liquid Copper and Partial Pressure of S_2 for the Copper-Matte Equilibrium

Temperature (°C)	Mole Fraction of S in Matte		Mole Fraction of S in Cu		$P(S_2)$, Atm	
	Experiment[26]	Calculated	Experiment[26]	Calculated	Experiment[26]	Calculated
1150	0.3260	0.3260	0.0251	0.0235	$4.06 \cdot 10^{-6}$	$3.69 \cdot 10^{-6}$
1200	0.3245	0.3245	0.0288	0.0292	$9.75 \cdot 10^{-6}$	$8.97 \cdot 10^{-6}$
1250	0.3230	0.3230	0.0349	0.0367	$2.15 \cdot 10^{-5}$	$2.05 \cdot 10^{-5}$

Table III. The Thermodynamic Properties of the Matte Phase

Pure Component	Reference for G^o	Stability Parameter, J/mol
Cu (liquid)	14	6130
Fe (liquid)	14	—
S (liquid)	15	—
Excess Parameters	**Value, J/mol**	
Cu-S system	Ref. 42	
Fe-S system	Ref. 42	
$\omega^{00}_{\text{Cu-Fe}}$	88,543	
$\omega^{10}_{\text{Cu-Fe}}$	$155{,}421 - 160.073\ T$	
$\omega^{20}_{\text{Cu-Fe}}$	$-382{,}016 + 217.883\ T$	

Table IV. The Thermodynamic Properties of the Slag Phase*

Excess Parameters	Value, J/mol
$CaO\text{-}FeO\text{-}Fe_2O_3\text{-}SiO_2$ system	Ref. 49
$\omega^{00}_{CuO_{1/2}-SiO_2}$	−8000
$\omega^{01}_{CuO_{1/2}-SiO_2}$	97,900
$\omega^{06}_{CuO_{1/2}-SiO_2}$	670,000
$\omega^{00}_{CuO_{1/2}-FeO}$	39,748
$\omega^{00}_{CuO_{1/2}-FeO_{3/2}}$	39,748
$\omega^{00}_{CuO_{1/2}-CaO}$	−23,540
$\omega^{01}_{CuO_{1/2}-CaO}$	11,455
$\omega^{011}_{FeO\text{-}SiO_2(CuO_{1/2})}$	−98,008
$\omega^{001}_{FeO\text{-}SiO_2(CuO_{1/2})}$	$40.107T$
$\omega^{001}_{CuO_{1/2}-FeO(CaO)}$	167,360

*Thermodynamic properties of pure liquid components CaO, FeO, Fe_2O_3, SiO_2, Cu_2O, CaS, FeS, and Cu_2S are taken from the FACT database.[14]

because Cu and Fe in the matte almost never form pairs with each other but are surrounded by sulfur ions. However, it was necessary to introduce a number of binary parameters, which describe roughly the Cu-Fe liquid, into the matte phase for technical reasons in order to provide a smooth extrapolation of the thermodynamic properties outside the composition range of the matte. These are listed as the three $\omega^{ij}_{\text{Cu-Fe}}$ parameters in Table III.

The phase equilibria between liquid alloy and the matte and between liquid alloy, matte, and γFe in the Cu-Fe-S system were studied by Krivsky and Schuhmann[44] and by Bale and Toguri.[26] One small ternary parameter $\omega^{001}_{\text{Cu-S(Fe)}}$ for the alloy phase was introduced to represent the data satisfactorily and to give reasonable extrapolations. The value of this parameter is listed in Table I. The notation of References 7 through 9 is used for parameters of the quasichemical model throughout this article.

III. Cu-Au AND Cu-O SYSTEMS

Thermodynamic properties and the phase diagram of the Cu-Au system were reviewed and assessed by Hultgren *et al.*[45] and Okamoto *et al.*[46] Experimental data selected from these assessments were optimized in the present study, with more weight given to the measurements of the activities of copper. The three $\omega^{ij}_{\text{Au-Cu}}$ parameters listed in Table I were necessary to obtain a good fit of the data.

When a Cu-Au alloy is used to control the copper activity for the matte-slag equilibria, only very small amounts of other components are present in the alloy. Hence, it is not required for purposes of the present study to optimize the other subsystems with gold such as Fe-Au.

The activities of oxygen in liquid copper were reviewed and assessed by Schmid[47] and Neumann *et al.*[48] The two $\omega^{ij}_{\text{Cu-O}}$ parameters of the quasichemical model listed in Table I were used to describe these data at 1200 °C to 1300 °C. Since the liquid metal phase of interest for copper smelting and converting is almost pure copper, it is not necessary to consider any other binary subsystems with oxygen in order to describe the solubility of oxygen in blister copper.

IV. SLAG

The quasichemical model is used to describe the thermodynamic properties of the slag. All available thermodynamic and phase equilibrium data for the $CaO\text{-}FeO\text{-}Fe_2O_3\text{-}SiO_2$ system have recently been optimized.[49] The oxygen pressures considered in the present study vary from 10^{-12} to 10^{-3} atm. This completely covers the range of oxygen potentials that may be of interest for the production of copper. Under these reducing conditions, the presence of Cu^{2+} in the slag can be neglected, so that all copper in the slag is assumed to be Cu^+.

Thermodynamic properties and phase diagram data for the binary systems of Cu_2O with CaO, FeO, Fe_2O_3, and SiO_2 were critically assessed and optimized by Dessureault.[13] The seven binary $\omega^{ij}_{\text{A-B}}$ parameters of the quasichemical model listed in Table IV were obtained, with $Z_{CuO_{1/2}} = 0.6888$ and the Gibbs energy of liquid Cu_2O taken from JANAF.[43]

A. *Copper Content in Fayalite Slag*

The solubility of copper in the slag has been reported in numerous publications, which can be divided into two major groups: studies in the sulfur-free $Cu_2O\text{-}CaO\text{-}FeO\text{-}Fe_2O_3\text{-}SiO_2$ system[50–61] and laboratory slag-matte equilibrium studies.[4,5,62–72] The last group shows a large scatter because of experimental difficulties in studying these multiphase

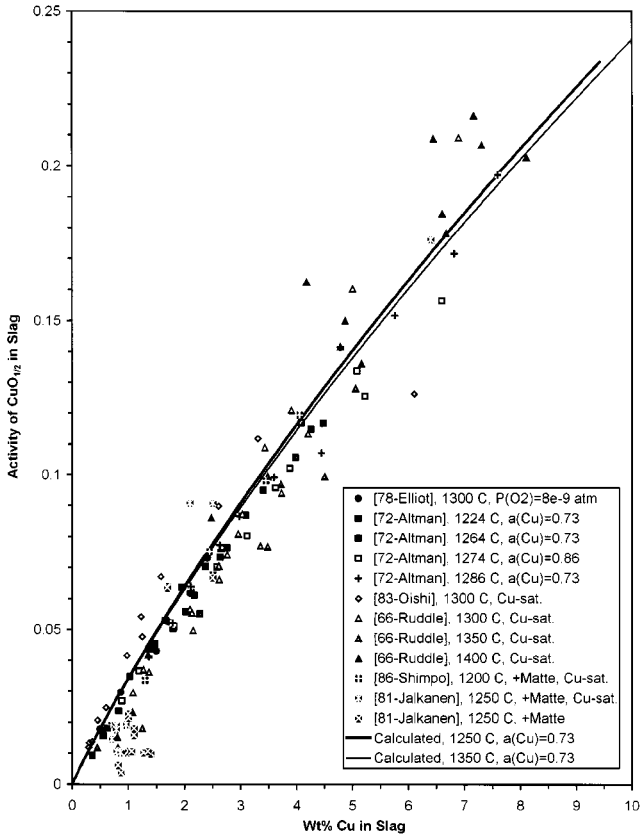

Fig. 1—Solubility of Cu in slag in equilibrium with Cu-Au alloys, or pure Cu, and SiO_2 at controlled O_2 potentials.

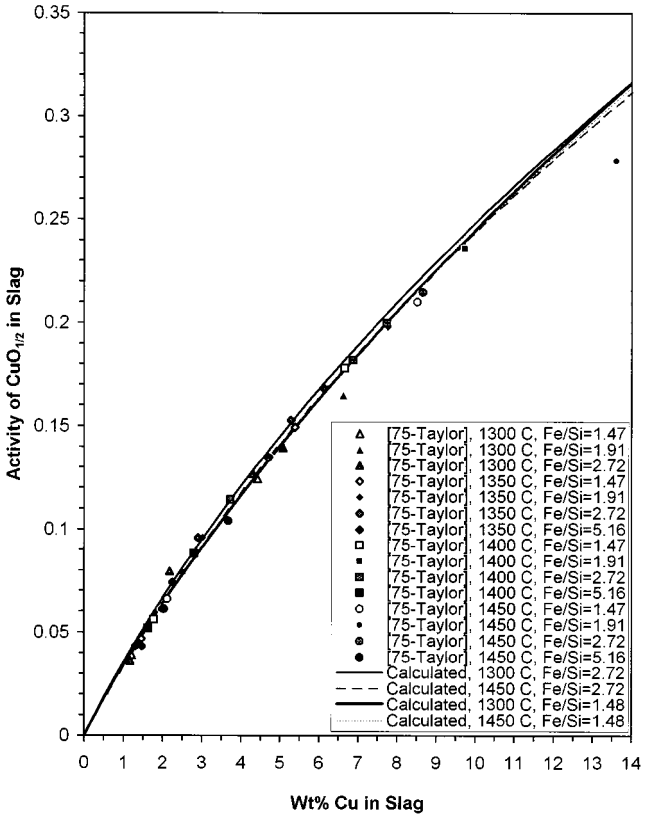

Fig. 2—Solubility of Cu in the slag in equilibrium with a Cu-Au alloy with activity of copper = 0.96 at controlled oxygen potentials.

systems, such as problems with sampling, quenching, and analysis of compositions of the phases. Entrainment of matte in the slag is also a well-known problem that affects the accuracy of these measurements.

1. *Solubility of copper in sulfur-free slag*

Some experiments[50,53,54,58–61] were performed in silica crucibles and correspond to SiO_2-saturated slags. Other studies[51,52,56,57] were performed in alumina crucibles, and the resultant slags contained substantial amounts of Al_2O_3. Since Al_2O_3 is not taken into account in the present study, these data were not used in the optimizations. Taylor and Jeffes[55] applied the levitation melting technique, which made it possible to study the effect of the Fe to Si ratio in the slag on the solubility of copper.

The activity of copper during experiments was controlled either by equilibration with liquid copper[50,60,61] or with Cu-Au alloy.[53,55,58,59] The oxygen potential was usually fixed by a flow of a CO/CO_2 gas mixture.

Careful analysis of the available experimental data for the Cu_2O-FeO-Fe_2O_3-SiO_2 system revealed that, although the data show significant scatter and cannot be directly compared to each other because they correspond to different temperatures, activities of copper, and oxygen and Fe/Si ratios in the slag, they all fall on the same curve when plotted in coordinates of activity of $CuO_{1/2}$ *vs* wt pct copper in the slag. Within the scatter of the experimental data, no systematic dependence on temperature (1225 °C to 1450 °C), Fe/Si ratio (1.3 to 5.0), oxygen partial pressure (10^{-5} to 2×10^{-12} atm), or activity of copper (0.07 to 1) is evident (Figures 1 and 2). All these effects are included in the activity of $CuO_{1/2}$, which is the driving force for the dissolution of copper in the slag. This fact makes the experimental data much more reliable and to some extent compensates experimental errors. Therefore, only those studies where copper and oxygen potentials are known and where the activity of $CuO_{1/2}$ can be calculated were used for optimization.

The two ternary $\omega^{ijk}_{\text{FeO-SiO}_2\text{(CuO}_{1/2}\text{)}}$ parameters listed in Table IV were added to reproduce all the experimental data. As can be seen from Figures, 1 and 2, all the data are described within experimental error limits.

The effect of additions of 4 to 11 wt pct lime on the solubility of copper in silica-saturated slag was studied by Altman,[58] by Elliot *et al.*,[59] and by Kim and Sohn.[61] The latter authors reported activities of $CuO_{1/2}$ both for the CaO-free and CaO-containing slags. Their activities at high concentrations of copper in the slag are considerably higher than obtained in the other studies.[50,53–55,58–60] The curvature of their plot of activity of $CuO_{1/2}$ *vs* wt pct Cu in the slag is also different from the other studies. Therefore, these data were not taken into account for the present optimization.

Figure 3 shows that CaO reduces the copper content of the slag. To reproduce these data, one more ternary parameter was introduced. This is the $\omega^{001}_{\text{CuO}_{1/2}\text{-FeO(CaO)}}$ parameter listed in Table IV.

2. *Copper content of slag in equilibrium with matte*

The solubilities of copper as a function of matte grade are summarized in Figures 4 and 5. The data are significantly scattered. When the matte grade (wt pct Cu in matte) approaches 80 pct, the solubility of copper sharply increases. In this region, the accuracy of the measurements of the

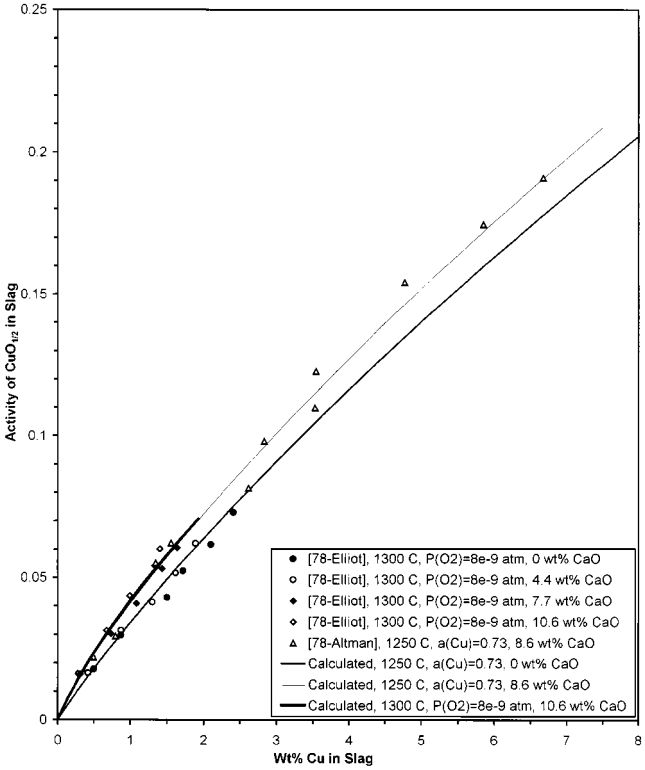

Fig. 3—Effect of additions of CaO on solubility of Cu in slag in equilibrium with Cu-Au alloys and SiO_2 at controlled oxygen potentials.

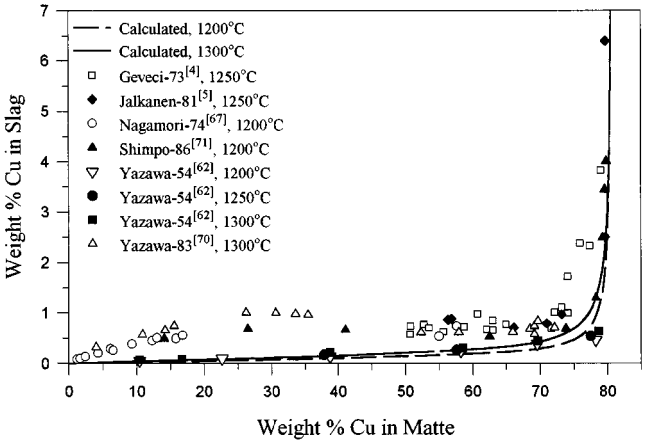

Fig. 4—Copper content of silica-saturated slag in equilibrium with matte and liquid copper or gamma-iron.

matte grade is not sufficient to define the corresponding Cu content.

The other significant disagreement among the measured copper contents occurs at matte grades around 30 pct in Figure 4 at γ-Fe saturation. This has caused controversy in the literature about the forms of copper in slag. The maximum in the reported copper solubility near 30 pct in Figure 4 was attributed to the presence of "Cu_2S" in the slag.[67,70,71] This assumption was questioned by Sridhar *et al.*[1] The solubilities calculated in the present study are in excellent agreement with the early work of Yazawa and Kameda[62] and the measurements of Tavera and Davenport,[68] but are lower than those obtained in the other studies.[67,70,71] The

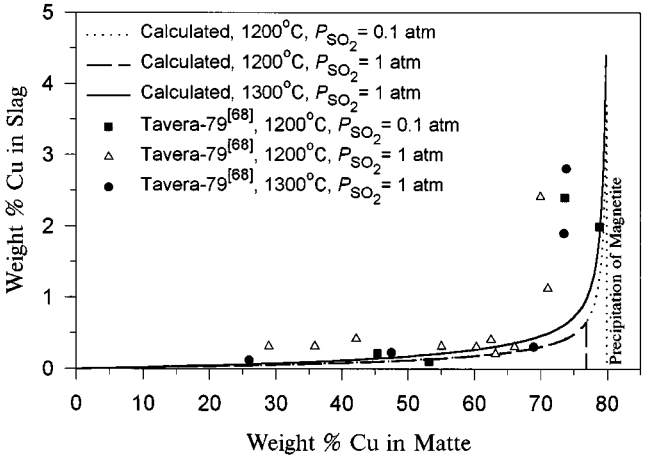

Fig. 5—Copper content of silica-saturated slag in equilibrium with matte at fixed pressure of SO_2.

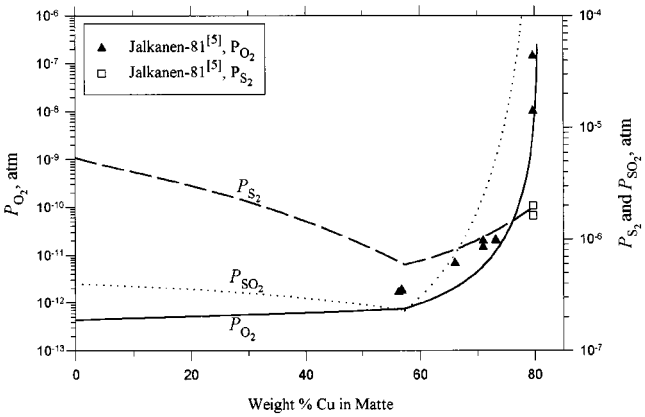

Fig. 6—Calculated partial pressures of O_2, S_2, and SO_2 over silica-saturated slag in equilibrium with matte and liquid copper or gamma-iron at 1250 °C (lines are calculated; points are experimental).

experimental disagreements in Cu solubility are most likely explained by suspensions of matte and slag in each other. At the low oxygen potentials associated with γ-Fe saturation (Figure 6), the matte and slag are, in fact, one oxysulfide phase with a miscibility gap. The similarity of these two liquids makes formation of such suspensions more probable. The other possible explanation is systematic errors in the analysis of small amounts of Cu. On the other hand, the calculations are also less accurate for the lower matte grades and oxygen partial pressures, because oxygen becomes progressively more soluble in the matte under these conditions, and oxygen solubility in the matte was not taken into account in the present study.

In any case, as pointed out by Sridhar *et al.*,[1] the solubilities of Cu obtained at γ-Fe saturation probably do not have much relevance for the understanding of copper losses in slag in industrial practice, because oxygen potentials used in plant practice are at least two orders of magnitude higher.

The calculated partial pressures of O_2, S_2, and SO_2 for SiO_2/slag/matte equilibria at γ-Fe and Cu saturation are shown in Figure 6. The agreement with the experimental data of Jalkanen[5] is believed to be within the accuracy of the experiments, even though these data were not used in the optimization. The Fe/SiO_2 ratio for these equilibria does

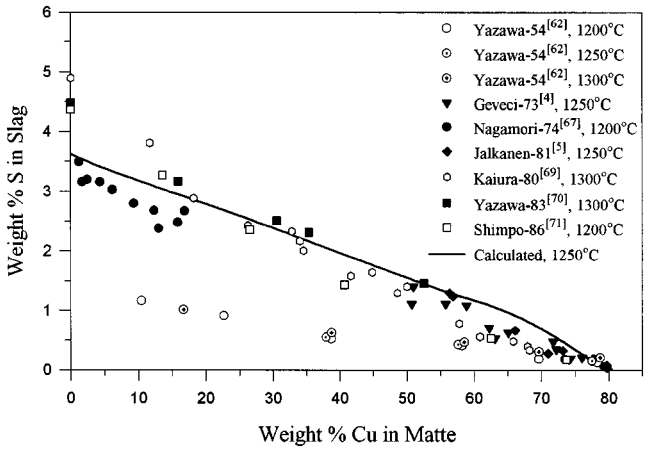

Fig. 7—Sulfur content of silica-saturated slag in equilibrium with matte and liquid copper or gamma-iron.

not vary greatly and is about 1.45, 1.3, and 1.2 wt pct at 1200 °C, 1250 °C, and 1300 °C, respectively.

In the present study, the optimizations are based on experimental data in sulfur-free systems. It is assumed that these data represent well the solubility of copper in the slag, and that it is not necessary to use the less accurate data obtained for matte-slag equilibria. This conclusion is supported by experimental data[5,71] for the matte-slag equilibria, where the activities of copper and oxygen were measured so that it was possible to calculate the activity of Cu_2O. As can be seen from Figure 1, these points fall on the activity-composition curve obtained for the sulfur-free system.

B. *Sulfur Content of Slag*

The Reddy–Blander model for sulfide capacities of multicomponent slags, as modified by Pelton *et al.*,[10] was used to calculate the solubility of sulfur in fayalite slag from a knowledge of the thermodynamic activities of the component oxides, with no adjustable parameters. The Gibbs energies of pure liquid FeS and Cu_2S were taken from the FACT database.[14]

The solubilities of sulfur in slag in equilibrium with matte as a function of matte grade are summarized in Figures 7 through 9. These results are at variance with one another and show a large scatter. The calculated lines are generally in good agreement with experimental data. Similarly, good agreement was obtained with the data[69,70] on the sulfur content of silica-saturated slag in equilibrium with matte at 1300 °C and $P_{SO_2} = 0.01$ atm.

The data of Yazawa and Kameda[62] are much lower than the other studies. On the other hand, the data of Sehnalek and Imris[65] (not shown in Figures 7 through 9) are higher, although the scatter of these data is very large. The data of Tavera and Davenport[68] (also not shown on Figures 7 through 9) are widely scattered as well, but are in agreement with the calculations within experimental error limits. The data for the sulfur solubilities at copper saturation reported by Jalkanen[5] (Figure 7), are in good agreement with the calculations. However, the data by the same author for unsaturated mattes in equilibrium with various gas atmospheres are somewhat higher than the calculations (Figure 9). The

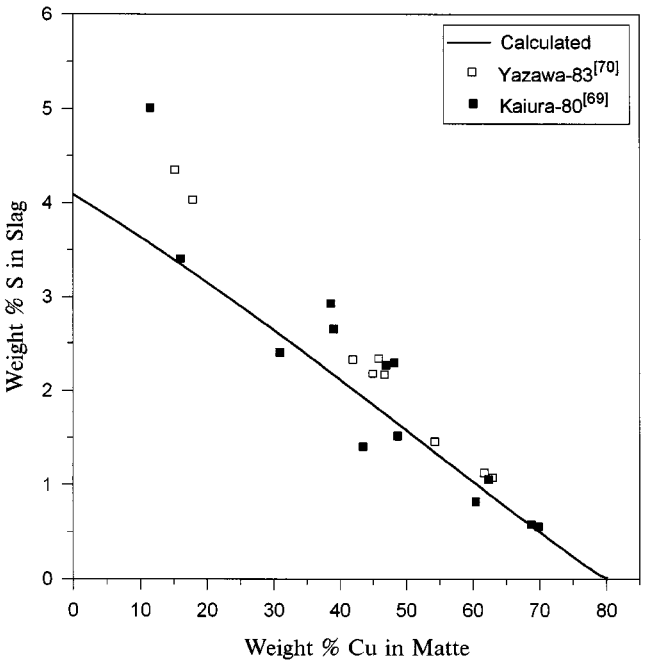

Fig. 8—Sulfur content of silica-saturated slag in equilibrium with matte at 1300 °C and $P_{SO_2} = 0.1$ atm.

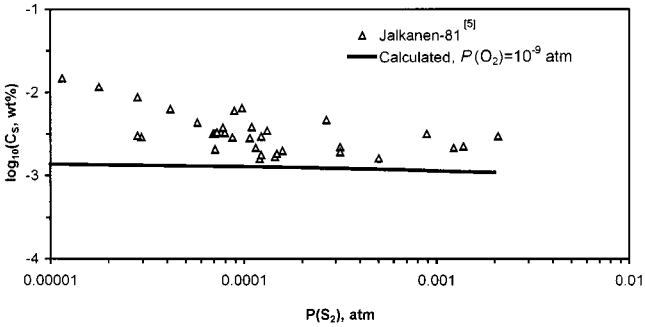

Fig. 9—Sulfide capacities in SiO_2-saturated slag in equilibrium with matte at 1250 °C.

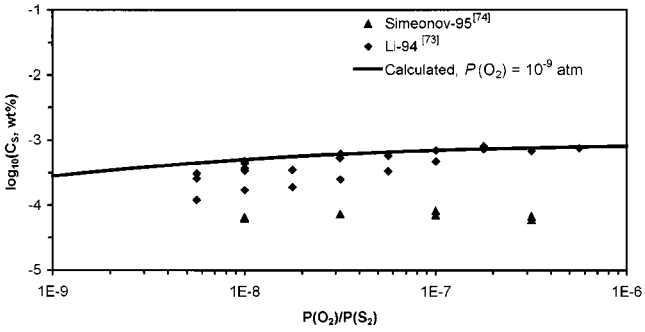

Fig. 10—Sulfide capacities in Cu-free SiO_2-saturated fayalite slag at 1200 °C.

sulfide capacity of slag shown on this plot is defined as

$$C_S = (\text{wt pct S})\left(\frac{P_{O_2}}{P_{S_2}}\right)^{1/2}$$

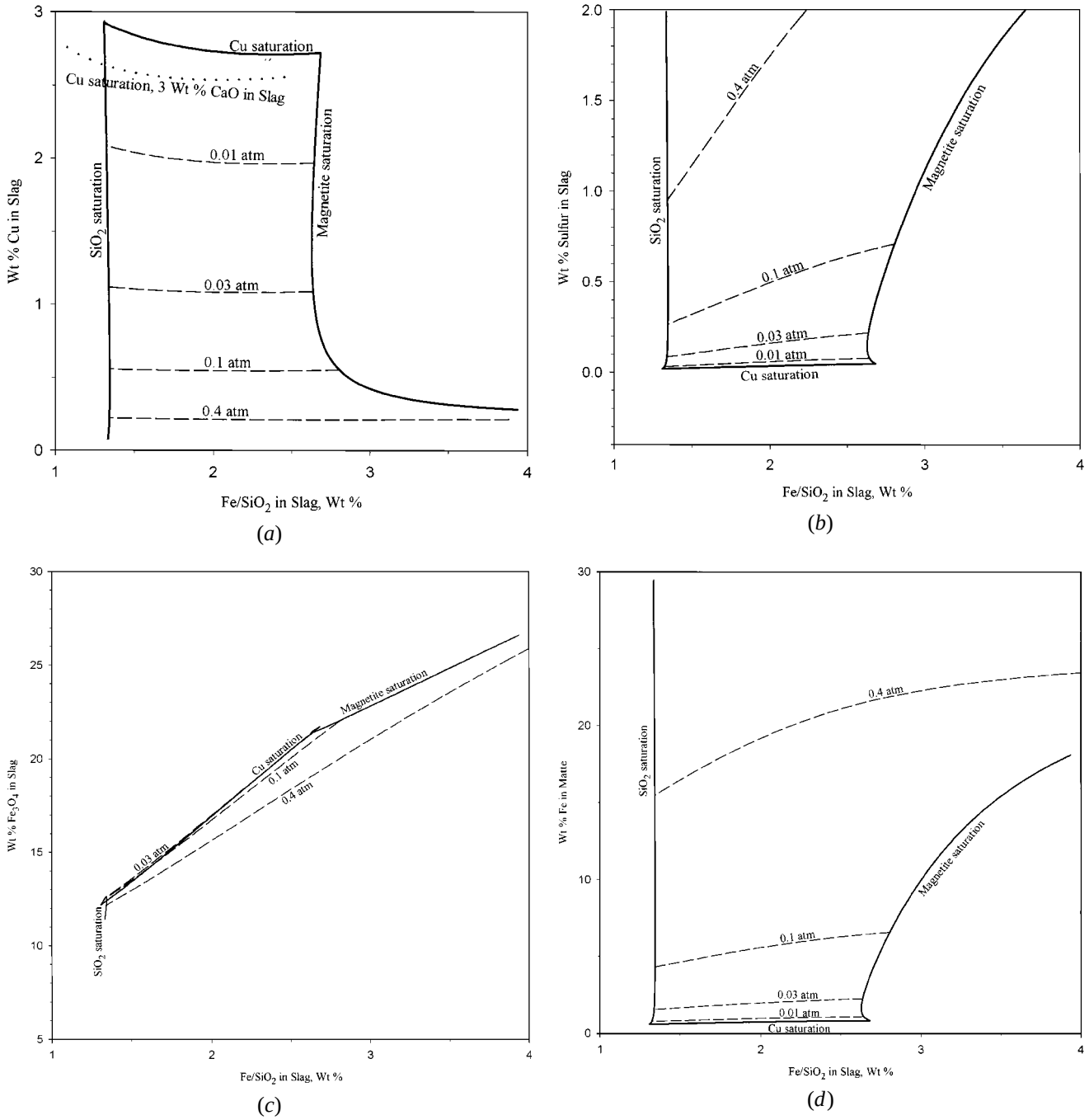

Fig. 11—(*a*) Copper content of slag in equilibrium with matte at 1250 °C and $P_{O_2} = 10^{-8}$ atm. Dashed lines are SO_2 isobars. (*b*) Sulfur content of slag in equilibrium with matte at 1250 °C and $P_{O_2} = 10^{-8}$ atm. Dashed lines are SO_2 isobars. (*c*) "Magnetite content" of slag in equilibrium with matte at 1250 °C and $P_{O_2} = 10^{-8}$ atm. Dashed lines are SO_2 isobars. (*d*) Iron content of matte in equilibrium with slag at 1250 °C and $P_{O_2} = 10^{-8}$ atm. Dashed lines are SO_2 isobars.

Sulfide capacities were also studied for Cu-free slags, which were not equilibrated with matte.[73,74] These data are shown in Figure 10. The calculated capacities are in agreement with Li and Rankin[73] but higher than those of Simeonov *et al.*[74]

From the aforesaid, the conclusion is drawn that the sulfur solubility in the slag is predicted by the model within the accuracy of the available experimental data, and that there is no need to introduce any adjustable parameters to describe these data.

V. CALCULATED MATTE-SLAG EQUILIBRIA

Finding an appropriate container material has always been one of the major problems in laboratory studies of matte-slag equilibria. Most of the work has been performed in iron, alumina, or silica crucibles. Therefore, many data are available at Fe saturation, although, as mentioned previously, these data do not correspond to common plant conditions. The use of alumina crucibles results in contamination of the slag with up to 10 pct Al_2O_3. Studies in silica crucibles do

not permit the iron to silica ratio in the slag to be varied. There is only one work by Taylor and Jeffes[55] where the need for a container was eliminated by the levitation melting technique, and the solubility of copper was studied at different Fe to Si ratios in the sulfur-free system.

The thermodynamic database for the slag, matte, and liquid copper phases developed in the present study makes it easy to calculate matte-slag equilibria at any given conditions of interest for plant practice. For example, Figures 11(a) through (d) show the compositions of matte and slag equilibrated at 1250 °C and $P_{O_2} = 10^{-8}$ atm as functions of Fe to silica ratio in the slag. The field of the matte-slag two-phase equilibria is limited by SiO_2 and magnetite saturation at low and high Fe/SiO_2 ratios, respectively. The SO_2 isobars over the two-phase fields are also shown on the figures.

The most commonly used convention in copper smelting employs the weight percentage of magnetite in the slag (by formally including all Fe^{3+} in the "component" Fe_3O_4) to characterize the degree of oxidation of iron. The calculated concentration of Fe_3O_4 in the slag is given in Figure 11(c). It should be noted that this figure is not a true phase diagram in that a point on it does not represent a unique state of the system. For example, the isobar $P_{SO_2} = 0.1$ atm intersects with the curve of copper saturation, which corresponds to about 0.0055 atm SO_2. At the point of the intersection, two different states of the system have the same Fe/SiO_2 ratio and concentration of Fe_3O_4 in the slag. Nevertheless, Figure 11(c) still shows how the wt pct Fe_3O_4 in the slag varies as a function of the iron to silica ratio at copper, magnetite, and silica saturation and along the SO_2 isobars.

The dotted line on Figure 11(a) corresponds to the matte-slag-copper equilibrium when the slag contains 3 wt pct lime. It covers the range from silica to magnetite saturation. As can be seen from the figure, the presence of CaO decreases the copper solubility in the slag by about half a percent. These figures can be of immediate interest for optimizing the conditions for the converting stage of copper production.

VI. CONCLUSIONS

In the present study, a self-consistent set of thermodynamic properties of the slag, matte, and liquid copper phases has been obtained based on all available thermodynamic and phase equilibrium data in the literature. The parameters of the quasichemical model for these three phases are summarized in Tables I, III, and IV. The database gives most accurate results for oxygen partial pressures from about 10^{-10} to 10^{-6} atm, sulfur pressures from 10^{-7} to 10^{-2} atm, temperatures from 1150 °C to 1350 °C, and matte grades above 50 wt pct Cu in the matte; that is, over the ranges of temperature, partial pressure, and matte grade encountered in modern industrial processes. At lower oxygen potentials and matte grades, matte and slag become increasingly soluble in each other. The modeling of matte and slag as one oxysulfide phase will be the subject of future work.

The modified quasichemical model was used for the slag, matte, and alloy phases. The sulfide solubility in the slag was predicted by the Reddy–Blander model, as modified by Pelton.

ACKNOWLEDGMENTS

Financial support from the Noranda Technology Center and from the Natural Science and Engineering Research Council of Canada is gratefully acknowledged.

REFERENCES

1. R. Sridhar, J.M. Toguri, and S. Simeonov: *Metall. Mater. Trans. B*, 1997, vol. 28B, pp. 191-200.
2. R. Sridhar, J.M. Toguri, and S. Simeonov: *JOM*, 1997, Apr., pp. 48-52.
3. F.Y. Bor and P. Tarassoff : *Can. Metall. Q.*, 1971, vol. 10 (4), pp. 267-71.
4. A. Geveci and T. Rosenqvist: *Trans. Inst. Min. Metall.*, 1973, vol. 82, pp. C193-C201.
5. H. Jalkanen: *Scand. J. Metall.*, 1981, vol. 10, pp. 177-84.
6. A.D. Pelton and M. Blander: *Metall. Trans. B*, 1986, vol. 17B, pp. 805-15.
7. S.A. Degterov and A.D. Pelton: *J. Phase Equilib.*, 1996, vol. 17 (6), pp. 476-87.
8. S.A. Degterov and A.D. Pelton: *J. Phase Equilib.*, 1996, vol. 17 (6), pp. 488-94.
9. S.A. Degterov and A.D. Pelton: *Metall. Mater. Trans. B*, 1997, vol. 28B, pp. 235-42.
10. A.D. Pelton, G. Erikson, and J.A. Romero-Serrano: *Metall. Trans. B*, 1993, vol. 24B, pp. 817-25.
11. P.A. Lindquist and B. Uhrenius: *CALPHAD*, 1980, vol. 4(3), pp. 193-200.
12. Y.Y. Chuang, R. Schmid, and Y.A. Chang: *Metall. Trans. A*, 1984, vol. 15A, pp. 1921-30.
13. Y. Dessureault: Ph.D. Thesis, Ecole Polytechnique de Montreal, Montreal, 1993.
14. A.D. Pelton, C.W. Bale, and W.T. Thompson: The FACT System, Ecole Polytechnique, Montreal, 1998 (http://www.crct.polymtl.ca).
15. R.C. Sharma and Y.A. Chang: *Metall. Trans. B*, 1979, vol. 10B, pp. 103-08.
16. W.R. Maddocks and G.E. Claussen: *Iron Steel Inst. Spec. Rep.*, 1936, vol. 14, pp. 97-124.
17. A. Hellawell and W. Hume-Rothery: *Phil. Trans. R. Soc. London*, 1957, vol. A249, pp. 417-59.
18. Y. Nakagawa: *Acta Metall.*, 1958, vol. 6, pp. 704-11.
19. A.A. Bochvar, A.S. Ekatova, E.V. Panchenko, and Y.F. Sidokhin: *Dokl. Akad. Nauk. SSSR*, 1967, vol. 174, pp. 863-64.
20. M. Hasebe and T. Nishizawa: *CALPHAD*, 1980, vol. 4, pp. 83-100.
21. W. Oelsen, E. Schurmann, and C. Florin: *Arch. Eisenhuttenwes.*, 1961; vol. 32, pp. 719-28.
22. A. El'Khasan, K. Abdel-Aziz, A.A. Vertman, and A.M. Samarin: *Izv. Akad. Nauk SSSR, Metally*, 1966, vol. 3, pp. 19-30.
23. F. Woolley and J.F. Elliott: *Trans. TMS-AIME*, 1967, vol. 239, pp. 1872-83.
24. Y. Tozaki, Y. Iguchi, S. Ban-ya, and T. Fuwa: *Chemical Metallurgy of Iron and Steel*, Iron and Steel Institute, London, 1973, pp. 130-32.
25. J.P. Morris and G.R. Zellars: *Trans. AIME*, 1956, vol. 206, pp. 1086-90.
26. C.W. Bale and J.M. Toguri: *Can. Metall. Q.*, 1976, vol. 15 (4), pp. 305-08.
27. C.W. Bale and J.M. Toguri: *J. Thermal Anal.*, 1971, vol. 3, pp. 153-67.
28. K. Sudo: *Sci. Rep. Res. Inst. Tohoku Univ. A*, 1950, vol. 2, pp. 519-30.
29. C.B. Alcock and F.D. Richardson: *Acta Metall.*, 1958, vol. 6, pp. 385-95.
30. J. Koh and A. Yazawa: *Tohoku Daigaku Senko Seiren Kenkysho Iho*, 1982, vol. 65 (7–8), pp. 567-78.
31. R. Schuhmann, Jr. and O.W. Moles: *TMS-AIME*, 1951, vol. 191, pp. 235-41.
32. K. Sudo: *Tohoku Daigaku Senko Seiren Kenkyusho Iho*, 1954, vol. 10, pp. 45-56.
33. K. Friedrich and M. Waehlert: *Metall. Erz.*, 1913, vol. 10, pp. 976-79.
34. M. Moulki and J. Osterwald: *Z. Metallkd.*, 1979, vol. 70 (12), pp. 808-10.
35. J. Chipman and Ta Li: *Trans. Am. Soc. Met.*, 1937, vol. 25, p. 435.
36. C.B. Alcock and L.L. Cheng: *J. Iron Steel Inst. London*, 1960, vol. 195, pp. 169-73.
37. S. Hayashi and T. Uno: *Tetsu-to-Hagane*, 1982, vol. 68, pp. 1728-1736.
38. M.R. Baren and N.A. Gokcen: in *Advances in Sulfide Smelting*, H.Y. John, D.B. George, and A.D. Zunkel, eds., AIME, Warrendale, PA, 1983, pp. 41-56.

39. C.W. Sherman, H.I. Elvander, and J. Chipman: *TMS-AIME*, 1950, vol. 188, pp. 334-40.
40. F. Ishii and T. Fuwa: *Tetsu-to-Hagane*, 1981 vol. 33, pp. 261-68.
41. S. Ban-ya and J. Chipman: *TMS-AIME*, 1968, vol. 242, pp. 940-46.
42. F. Kongoli, Y. Dessureault, and A.D. Pelton: *Metall. Mater. Trans. B*, 1998, vol. 29B, pp. 591-601.
43. M.W. Chase, C.A. Davies, J.R. Downey, D.J. Frurip, R.A. McDonald, and A.N. Syverud: *JANAF Thermochemical Tables*, 3rd ed., *J. Phys. Chem. Ref. Data*, 1985, vol. 14, suppl. 1.
44. W.A. Krivsky and R. Schuhmann, Jr.: *J. Met.*, 1957, vol. 9, pp. 981-88.
45. R. Hultgren, P.D. Desai., D.T. Hawkins, M. Gleiser, and K.K. Kelley: *Selected Values of the Thermodynamic Properties of Binary Alloys*, ASM, Metals Park, OH, 1973.
46. H. Okamoto, D.J. Chakrabarti, D.E. Laughlin, and T.B. Massalski: *Bull. Alloy Phase Diag.*, 1987, vol. 8 (5), pp. 454-74.
47. R. Schmid: *Metall. Trans. B*, 1983, vol. 14B, pp. 473-81.
48. J.P. Neumann, T. Zhong, and Y.A. Chang: *Bull. Alloy Phase Diagrams.*, 1984, vol. 5 (2), pp. 136-40.
49. P. Wu: *Ph.D. Thesis*, Ecole Polytechnique de Montreal, Montreal, 1992.
50. R.W. Ruddle, B. Taylor, and A.P. Bates: *Trans. Inst. Min. Metall.*, 1966, vol. 75, pp. C1-C12.
51. J.M. Toguri and N.H. Santander: *Can. Metall. Q.*, 1969, vol. 8, pp. 167-71.
52. J.M. Toguri and N.H. Santander: *Metall. Trans.*, 1972, vol. 3, pp. 586-88.
53. R. Altman and H.H. Kellogg: *Trans. Inst. Min. Metall.*, 1972, vol. 81, pp. C163-C175.
54. J.B.W. Bailey and F.A. Garner: *Minerals Sci. Eng.*, 1974, vol. 6 (2), pp. 106-17.
55. J.R. Taylor and J.H.E. Jeffes: *Trans. Inst. Min. Metall.*, 1975, vol. 84, pp. C18-C24.
56. M. Nagamori, P.J. Mackey, and P. Tarassoff: *Metall. Trans. B*, 1975, vol. 6B, pp. 295-301.
57. M. Nagamori and P.J. Mackey: *Metall. Trans. B*, 1977, vol. 8B, pp. 39-46.
58. R. Altman: *Trans. Inst. Min. Metall.*, 1978, vol. 87, pp. C23-C28.
59. J. Elliot, J.B. See, and W.J. Rankin: *Trans. Inst. Min. Metall.*, 1978, vol. 87, pp. C204-C211.
60. T. Oishi, M. Kamuo, K. Ono, and J. Moriyama: *Metall. Trans. B*, 1983, vol. 14B, pp. 101-04.
61. H.G. Kim and H.Y. Sohn: *Metall. Mater. Trans. B*, 1998, vol. 29B, pp. 583-90.
62. A. Yazawa and M. Kameda: *Technol. Rep. Tohoku Univ.*, 1954, vol. 19(1), pp. 1-22.
63. P. Spira and N. Themelis: *J. Met.*, 1969, vol. 21 (4), pp. 35-42.
64. E.-B. Johansen, T. Rosenqvist, and P.T. Torgersen: *J. Met.*, 1970, vol. 22 (10), pp. 39-47.
65. F. Sehnalek and I. Imris: in *Advances in Extractive Metallurgy and Refining*, M.J. Jones, ed., IMM, London, 1972, pp. 39-62.
66. U. Kuxmann and H. Bussman: *Erzmetallurgy*, 1974, vol. 27 (7–8), pp. 353-65.
67. M. Nagamori: *Metall. Trans. B*, 1974, vol. 5B, pp. 531-38.
68. F.J. Tavera and W.G. Davenport: *Metall. Trans. B*, 1979, vol. 10B, pp. 237-41.
69. G.H. Kaiura, K. Watanabe, and A. Yazawa: *Can. Metall. Q.*, 1980, vol. 19 (2), pp. 191-200.
70. A. Yazawa, S. Nakazawa, and Y. Takeda: in *Advances in Sulfide Smelting*, H.Y. John, D.B. George, and A.D. Zunkel, eds., AIME, Warrendale, PA, 1983, pp. 99-117.
71. R. Shimpo, S. Goto, O. Ogawa, and I. Asakura: *Can. Metall. Q.*, 1986, vol. 25, pp. 113-21.
72. Y. Takeda: in *Metallurgical Processes for Early Twenty-First Century*, H.Y. Sohn, ed., The Minerals, Metals & Materials Society, Warrendale, PA, 1994, pp. 453-66.
73. H. Li and W.J. Rankin: *Metall. Mater. Trans. B*, 1994, vol. 25B, pp. 79-89.
74. S.R. Simeonov, R. Sridhar, and J.M. Toguri: *Metall. Trans. B*, 1995, vol. 26B, pp. 325-34.